

# Flow & Heat Transfer Characteristics In A Triangular Enclosure Filled With Hybrid Nanofluid Containing Heat Source /Sink In Bottom Wall

M. U. Ahammad, Abu Hanifa, Nazim Mahmud

Department of Mathematics, Dhaka University of Engineering and Technology, Gazipur, Bangladesh

---

## Abstract:

This analysis explores the consequences of flow and heat transfer by the process of free convection inside a triangular cavity, which contains heat source/sink at the bottom wall. The entire cavity has been filled with  $Al_2O_3$ -Cu water based hybrid nanofluid. Finite element method has been applied for discretization the governing equations of the present problem numerically. A fixed Prandtl number ( $Pr=0.71$ ) has been used for the numerical solution. The impact of relevant parameters such as Rayleigh number ( $Ra$ ), heat generation ( $Q$ ), Hartmann number and also variation of heat source/sink location has been studied. Outcomes of this research are represented by graphs and tables in order to identify the variations in velocity profile, temperature profile, as well as heat transfer rate for the studied cases that are exposed in terms of streamlines, isotherms and average Nusselt number respectively. Results exhibit that the average heat transfer rises with the increment of Rayleigh number whereas it decreases for the rising values of heat generating parameter and magnetic field parameter.

**Introduction:** The natural convection heat transfer process is broadly used in various designing systems because of its huge applications in geophysics, atomic reactor framework, cooling of hardware frame work, close planetary system, and so on. In the last few years, researchers have utilized numerous techniques for increasing heat-transfer coefficient. Hybrid nanofluid is one of those efficient mediums, which has higher heat conductivity rather than other nanofluids. It is one of the forms of nanotechnology that has become a topic of attraction because of its tremendous heat transfer performance in different sectors including cooling, defense, energy/power production, space, nuclear, microelectronics, and many other sectors. MHD natural convection in a triangular cavity filled with a Cu- $Al_2O_3$ /water hybrid nanofluid with localized heating from below and internal heat generation was studied by Rashad et al. [1]. Dogonchi et al. [2] investigated numerical analysis of natural convection of Cu- water nanofluid filling triangular cavity with semicircular bottom wall. Mahmoudi et al. [3] studied effect of magnetic field on natural convection in a triangular enclosure filled with nanofluid. Chamkha and Ismael [4] studied magnetic field effect on mixed convection in LID-driven trapezoidal cavities filled with a Copper–Water nanofluid with an aiding or opposing side wall. Analysis of hybrid nanofluid behavior in a triangular cavity along with heat source considering the effect of Magnetic force was presented by Angirasa [5]. Cu- $Al_2O_3$  hybrid nanofluid natural convection in an inclined enclosure with wavy walls partially layered by porous medium was studied by Kadhim et al. [6]. Buoyancy driven heat transfer enhancement in a two-dimensional enclosure utilizing nanofluids was carried out by Khanafer and Lightstone [7]. Numerical investigations on heat transfer characteristics of single particle and hybrid nanofluids in uniformly heated tubewas presented by Garud and Lee [8]. Experimental studies of nanofluid thermal conductivity enhancement and applications was analyzed by Tawfik [9]. The use of nanofluids for enhancing the thermal performance of stationary solar collectors was carried out by Muhammad et al. [10]. Review on nanofluids characteristics, heat transfer characterization and applications was analyzed by Raja et al. [11]. Botha et al. [12] studied physicochemical properties of oil based nanofluids containing hybrid structures of silver nanoparticle supported on silica. Effect of nanoparticles on critical heat flux of water in pool boiling heat transfer was carried by You et al. [13]. Tayebi et al. [14] investigated natural convection and entropy production in hybrid nanofluid filled-annular elliptical cavity with internal heat generation or absorption. The enhancement of effective thermal conductivity and effective dynamic viscosity of nanofluids was analyzed by Azmi et al. [15]. Brinkman [16] analyzed the viscosity of concentrated suspensions and solution. A treatise on electricity and magnetism was performed by Maxwell [17].

**Key Word:** Triangular Cavity, Nusselt Number, Hybrid Nanofluid, Rayleigh Number.

---

Date of Submission: 29-10-2023

Date of Acceptance: 09-11-2023

---

### I. Problem Description

The schematic diagram of the studied geometry is a right angle triangular enclosure of horizontal length  $L$ , and vertical length  $1.2L$ ; that is described in Figure 1. The enclosure has been filled with hybrid  $Al_2O_3$ -Cu/water nanofluid in the presence of internal heat generation. A heat source is located at the left side and a heat sink is placed at the right side of the bottom wall (each are of length  $L/2$ ), where the source/sink positions are changeable. Both of the vertical and inclined walls of the enclosure are considered as thermally isolated. A uniform external magnetic field has been imposed in the horizontal direction. It has been assumed that both the fluid and hybrid nanoparticles are in thermal equilibrium and there is no slip between them. Also, the base fluid and hybrid nanofluid properties (Table 1) are assumed constant except for the density variation, which is maintained on Boussinesq approximation.

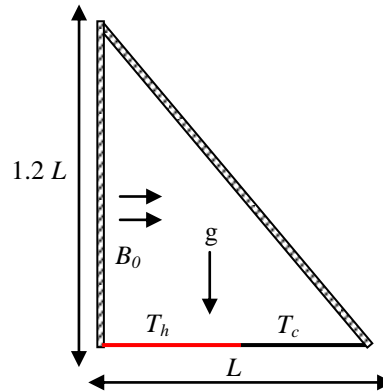


Figure 1: Schematic diagram of rectangular enclosure with heat source and sink

### II. Mathematical Formulation

The hybrid nanofluid used in the work has been considered as two-dimensional, steady, Newtonian, laminar and incompressible. The equations for the conservation of mass, momentum and energy in Cartesian coordinate system for hybrid nanofluid [1] are given below:

$$\frac{\partial U}{\partial X} + \frac{\partial V}{\partial Y} = 0 \quad (1)$$

$$U \frac{\partial U}{\partial X} + V \frac{\partial U}{\partial Y} = -\frac{\partial P}{\partial X} + Pr \left( \frac{\rho_f}{\rho_{hnf}} \right) \left( \frac{\mu_{hnf}}{\mu_f} \right) \left( \frac{\partial^2 U}{\partial X^2} + \frac{\partial^2 U}{\partial Y^2} \right) \quad (2)$$

$$U \frac{\partial V}{\partial X} + V \frac{\partial V}{\partial Y} = -\frac{\partial P}{\partial Y} + Pr \left( \frac{\rho_f}{\rho_{hnf}} \right) \left( \frac{\mu_{hnf}}{\mu_f} \right) \left( \frac{\partial^2 V}{\partial X^2} + \frac{\partial^2 V}{\partial Y^2} \right) - \left( \frac{\rho_f}{\rho_{hnf}} \right) \left( \frac{\sigma_{hnf}}{\sigma_f} \right) Ha^2 Pr V + \left( \frac{(\rho\beta)_{hnf}}{\rho_{hnf} \beta_f} \right) Ra Pr \theta \quad (3)$$

$$U \frac{\partial \theta}{\partial X} + V \frac{\partial \theta}{\partial Y} = \frac{\alpha_{hnf}}{\alpha_f} \left( \frac{\partial^2 \theta}{\partial X^2} + \frac{\partial^2 \theta}{\partial Y^2} \right) + \frac{(\rho C_p)_f}{(\rho C_p)_{hnf}} Q \quad (4)$$

where  $Pr = \frac{\rho_f \nu_f}{\alpha_f}$ ,  $Ra = \frac{g \beta_f q'' H^4}{\rho_f \alpha_f k_f}$ ,  $Ha = B_0 H \sqrt{\frac{\alpha_f}{\mu_f}}$  are the Prandtl number, Rayleigh number and the magnetic Hartmann number respectively and  $Q$  is the dimensionless heat generation parameter.

The equation (1) to (4) are made dimensionless by using the following relations

$$X = \frac{x}{H}, Y = \frac{y}{H}, U = \frac{uH}{\alpha_f}, V = \frac{vH}{\alpha_f}, \theta = \frac{T - T_c}{T_h - T_c}, P = \frac{pH^2}{\rho_{hnf} \alpha_f^2}, T_h - T_c = \frac{q'' H}{k_f}, Q = \frac{H}{q''} Q_0 \quad (5)$$

The boundary condition for the problem is given below:  
All the boundaries of the triangle:  $U = V = 0$ ,

On the left and inclined wall:  $\frac{\partial \theta}{\partial N} = 0$ ,

and on the left portion of bottom wall:  $\theta = 1$ , (Source)

whereas on the right portion of bottom wall:  $\theta = 0$ , (Sink)

The effective properties of Hybrid nanofluid ( $Al_2O_3$ -Cu/water) is defined as follows:

$$\text{density: } \rho_{hnf} = (1 - \phi_1)\rho_1 + \phi_2\rho_2 + \phi_3\rho_3, \text{ thermal diffusivity: } \alpha_{hnf} = \frac{k_{hnf}}{(\rho C_p)_{hnf}}$$

$$\text{heat capacitance: } (\rho C_p)_{hnf} = (1 - \phi_1)(\rho C_p)_1 + \phi_2(\rho C_p)_2 + \phi_3(\rho C_p)_3$$

$$\text{thermal expansion coefficient: } (\rho\beta)_{hnf} = (1 - \phi_1)(\rho\beta)_1 + \phi_2(\rho\beta)_2 + \phi_3(\rho\beta)_3$$

$$\text{viscosity based on Brinkman model [16]: } \mu_{hnf} = \frac{\mu_1}{(1 - \phi_2 - \phi_3)^{2.5}}$$

thermal conductivity, according to the Maxwell-Garnetts model [17]:

$$k_{hnf} = k_1 \left( \frac{\phi_2 k_2 + \phi_3 k_3}{\phi_1} + 2k_1 + 2(\phi_2 k_2 + \phi_3 k_3) - 2\phi_1 k_1 \right) \times \left( \frac{\phi_2 k_2 + \phi_3 k_3}{\phi_1} + 2k_1 - (\phi_2 k_2 + \phi_3 k_3) + \phi_1 k_1 \right)^{-1}$$

Effective electrical conductivity according to the Maxwell-Garnetts model [17]

$$\sigma_{hnf} = \sigma_1 \left( 1 + \frac{3 \left( \frac{\phi_2 \sigma_2 + \phi_3 \sigma_3}{\phi_1} - (\phi_2 \sigma_2 + \phi_3 \sigma_3) \right)}{\left( \frac{\phi_2 \sigma_2 + \phi_3 \sigma_3}{\phi_1} + 2 \right) - \left( \frac{\phi_2 \sigma_2 + \phi_3 \sigma_3}{\phi_1} - (\phi_2 \sigma_2 + \phi_3 \sigma_3) \right)} \right)$$

where  $\phi_1$  is the overall volume concentration of two different types of nanoparticles dispersed in hybrid nanoparticles and is calculated as  $\phi_1 = \phi_2 + \phi_3$ . Average Nusselt number at the heated wall of the enclosure is express as  $Nu_{av} = -\frac{k_{hnf}}{k_1} \int_0^{L/2} \frac{\partial \theta}{\partial X} dY$ , where  $L/2$  is length of the heated surface.

**Table 1:** Thermophysical properties of water, alumina and copper [1]

Property	Water	Alumina ( $Al_2O_3$ )	Copper (Cu)
$C_p$ ( $Jkg^{-1}K^{-1}$ )	4179	765	385
$\rho$ ( $kgm^{-3}$ )	997.1	3970	8933
$k$ ( $Wm^{-1}K^{-1}$ )	0.613	40	401
$\beta$ ( $K^{-1}$ )	$21 \times 10^{-5}$	$.85 \times 10^{-5}$	$1.67 \times 10^{-5}$
$\sigma$ ( $\mu S/m$ )	.05	$1 \times 10^{-10}$	$5.96 \times 10^7$

### III. Computational Procedure

Galerkin weighted residual based finite element method is applied to solve the dimensionless equation (1-4). In this method, the solution domain is discretized into meshes, which are fitted of non-uniform meshing elements (triangular, rectangular). Using the Galerkin weighted residual at the nodes of the elements, the governing partial differential equations are converted into a system of integral equations. Lastly, the basic unknown variables like velocity component U, V, temperature  $\theta$  and pressure P are obtained by the help of such converted equations along with the boundary condition (6). For the accuracy of the result grid test is required and code validation is also essential for confirmation the validity of the current code.

**Grid Independent Test:** For avoiding the complexity of the computational domain, at first grid refinement test is performed for this study. Different types of grid for two different cases (source/sink location) have been considered for the grid refinement analysis that are shown in Table 2 and Table 3. As the variations among the results for 12800 and 17162 are very negligible, 12800 elements are selected throughout the simulation.

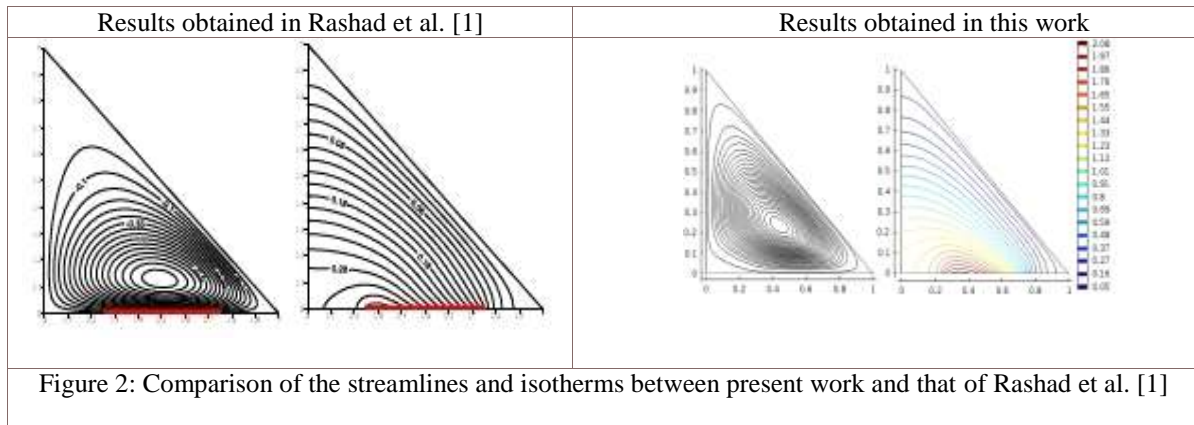
**Table no 2:** Average Nusselt number for the case of left heat source and right heat sink while  $\phi = 0.05, Q=1, Ha= 25$  and  $Ra = 10^6$

No. of elements	$Nu_h$	$Nu_c$
926	5.7852	7.1986
1459	5.9186	7.2800
4543	6.4710	7.6855
12800	6.9226	8.0598
17162	6.9231	8.0602

**Table no 3:** Average Nusselt number for the case of left heat sink and right heat source while  $\phi = 0.05, Q=1, Ha= 25$  and  $Ra = 10^6$

No. of elements	$Nu_h$	$Nu_c$
926	7.5607	6.1092
1459	7.6392	6.2460
4543	8.0340	6.8042
12800	8.4042	7.2586
17162	8.4043	7.2592

**Model Validation:** In order to justify the numerical code of present work, we have compared the streamlines and isotherms of present study with those of the previously published work Rashad et al. [1] which had done for triangular cavity with localized constant temperature gradient from bottom wall. The comparison is shown in Figure 2 that reveals a good agreement for the mentioned results and thus it makes an assertion of the current numerical code.



#### IV. Results And Discussions

The present investigation addresses a problem on the free convective two-dimensional hybrid nanofluid flow along with thermal field characteristics considering the effect of several pertinent parameters namely Rayleigh number, Heat generating parameter, Hartmann number, and location of heat source/sink (left and right). The value of Rayleigh number taken in the present work is  $10^3, 10^4, 10^5$  and  $10^6$ , whereas  $Q = 1, 2, 3, 4$ , and  $Ha = 0, 25, 50, 100$ . Mainly, two different cases- left sink, right source and left source, right sink at the bottom surface of the triangular cavity are analyzed in this work. Streamlines, isothermal lines, average Nusselt number at the hot wall and cold wall of horizontal side of the enclosure are used for the explanation of fluid flow and heat transfer phenomena.

##### Case 1: Left heated (source), Right cooled (Sink)

In a triangular enclosure with left portion heated (acting as a source) and the right portion cooled (acting as a sink) of the bottom wall, the fluid inside will experience natural convection. As the fluid near the heated side gets warm and less dense, it rises, creating a flow towards the cooler side. This, in turn, sets up a circulation pattern known as convection cells or streamlines. The isotherms, on the other hand, represent lines that connect points of equal temperature. In this case, the isotherms will be influenced by the heat input from the heated side and the heat removal at the cooled side. This case is described in Figure 2 and Figure 3.

##### **Effect of Rayleigh Number Ra**

Rayleigh Number (Ra) =  $10^3$ : At low Rayleigh numbers, the buoyancy forces are relatively weak compared to the viscous forces. The fluid flow will be primarily laminar and steady. The isotherms will be relatively smooth, and the streamlines will show organized and simple flow patterns. The convective heat transfer will be relatively weak compared to conductive heat transfer.

Rayleigh Number (Ra) =  $10^4$ : As the Rayleigh number increases, the buoyancy forces become more significant, and the flow may transition from laminar to a more complex pattern with multiple convection cells. The isotherms will start to show some irregularities, and the streamlines will become more distinct and may exhibit some vortices.

Rayleigh Number (Ra) =  $10^5$ : At this range of Rayleigh numbers, the buoyancy forces further increase, leading to more vigorous fluid motion and the formation of larger and more numerous convective cells. The isotherms will show more pronounced distortions, and the streamlines will exhibit more intricate flow patterns with multiple vortices and recirculation zones.

Rayleigh Number (Ra) =  $10^6$ : At high Rayleigh numbers, the buoyancy forces dominate the fluid behavior, leading to chaotic and turbulent flow patterns. The flow will be highly irregular with intense mixing and eddies. The isotherms will be highly distorted, and the streamlines will show complex and turbulent flow patterns.

##### **Effect of Heat Generating Parameter Q**

Heat Generating Parameter (Q)=1: At Q= 1, the heat generated within the enclosure is relatively low compared to the heat input from the heated side. The streamlines will primarily be driven by the temperature difference between the heated and cooled sides. The isotherms will show a gradual transition from the heated side to the cooled side, with relatively smooth contours. The effect of internal heat generation may not be prominent at this value of Q.

Heat Generating Parameter ( $Q$ ) = 2: As  $Q$  increases to 2, the heat generated within the enclosure becomes more significant. It starts to influence the fluid flow and temperature distribution. The streamlines may exhibit more complex patterns with the combined influence of the heat source and the temperature difference between the sides. The isotherms will show more variations and steeper temperature gradients within the enclosure.

Heat Generating Parameter ( $Q$ ) = 3: At  $Q = 3$ , the internal heat generation further enhances the impact on the fluid flow and temperature distribution. The streamlines may show turbulent behavior or the formation of multiple convection cells due to the increased heat input. The isotherms will exhibit irregularities and more pronounced temperature gradients, showing the influence of the heat source on the thermal field.

Heat Generating Parameter ( $Q$ ) = 4: At  $Q = 4$ , the internal heat generation is even higher. The fluid flow patterns will be significantly influenced by the heat generated within the enclosure. The streamlines may become highly irregular and turbulent, with multiple convection cells dominating the flow. The isotherms will exhibit even more pronounced temperature variations, reflecting the strong influence of the heat source.

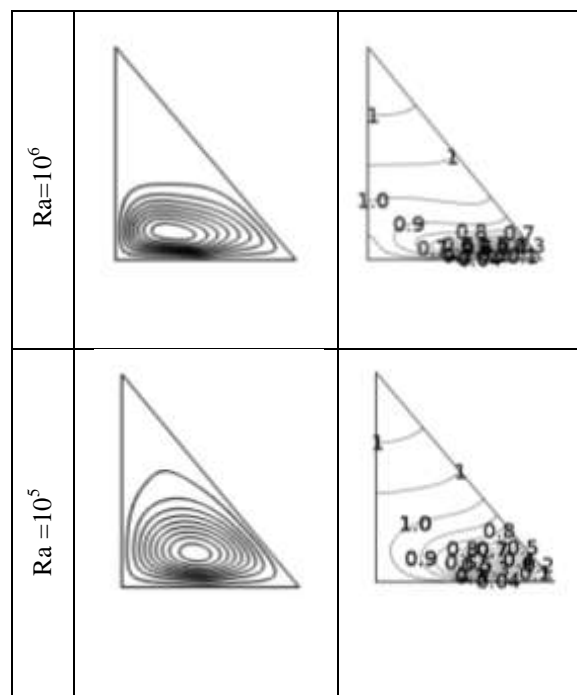
**Table no 4:** Average Nusselt number for variation of Ra (L heated, R cooled) while  $\phi = 0.05$ ,  $Q = 1$ , and  $Ha = 25$

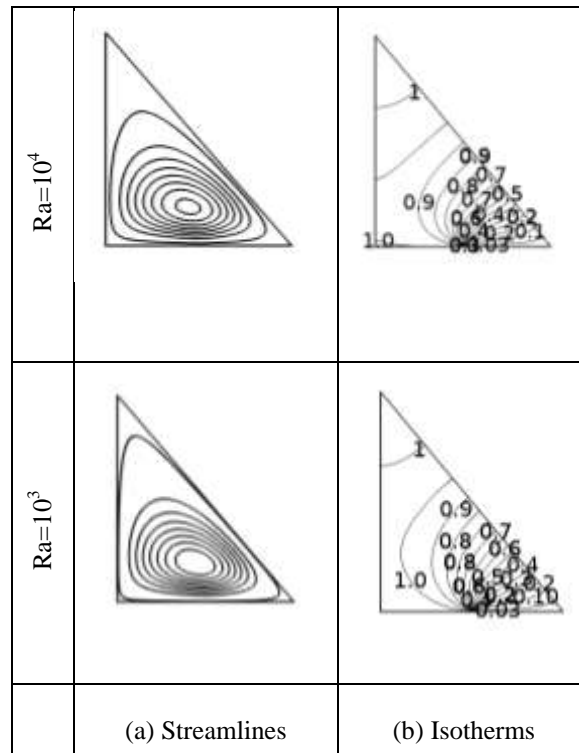
Ra	$Nu_h$	$Nu_c$
$10^3$	4.0267	5.0586
$10^4$	4.1027	5.1407
$10^5$	4.9198	5.9882
$10^6$	6.9226	8.0598

**Table no 5:** Average Nusselt number for variation of  $Q$  (L heated, R cooled) while  $\phi = 0.05$ ,  $Ha = 25$ , and  $Ra = 10^6$

$Q$	$Nu_h$	$Nu_c$
1	6.9226	8.0598
2	6.3413	8.5095
3	5.7962	8.9781
4	5.3882	9.4671

Table 4 and 5 shows the average Nusselt number for the different values of Ra and  $Q$  respectively. From these tables it is observed that  $Nu_{av}$  increases for the rising values of Ra and  $Q$  but an reverse effect is found for heat generating parameter and heat source case.





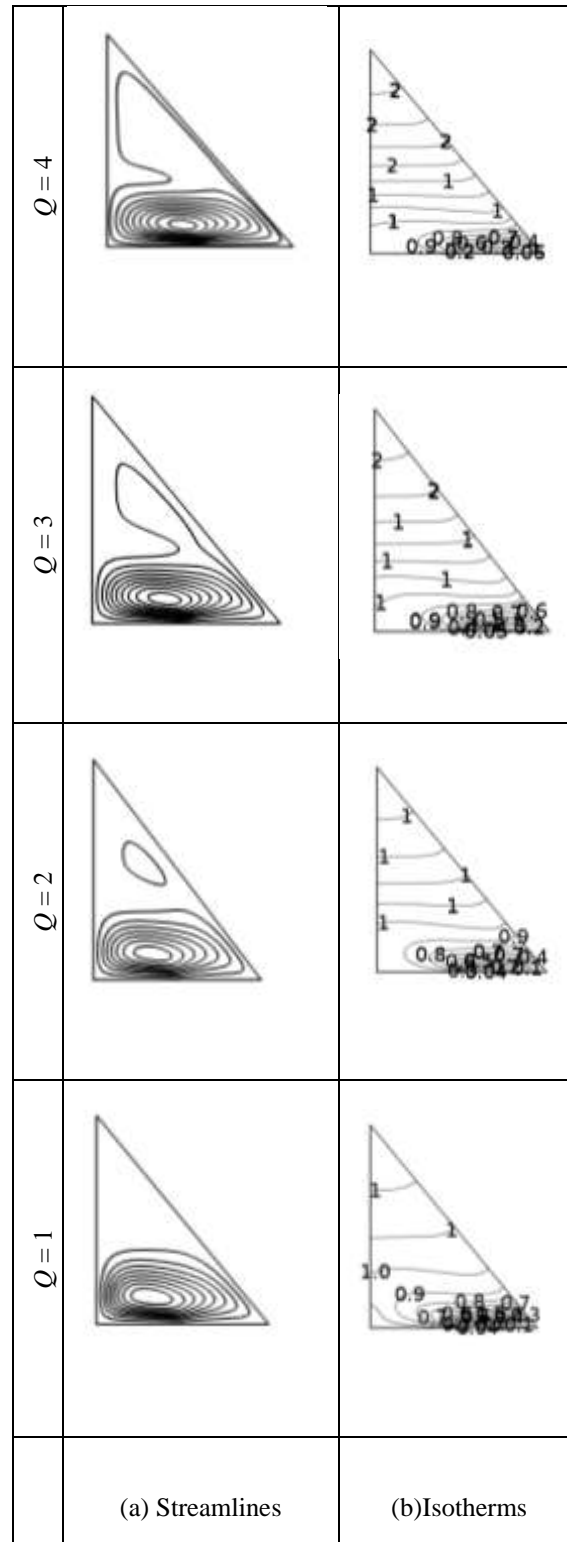
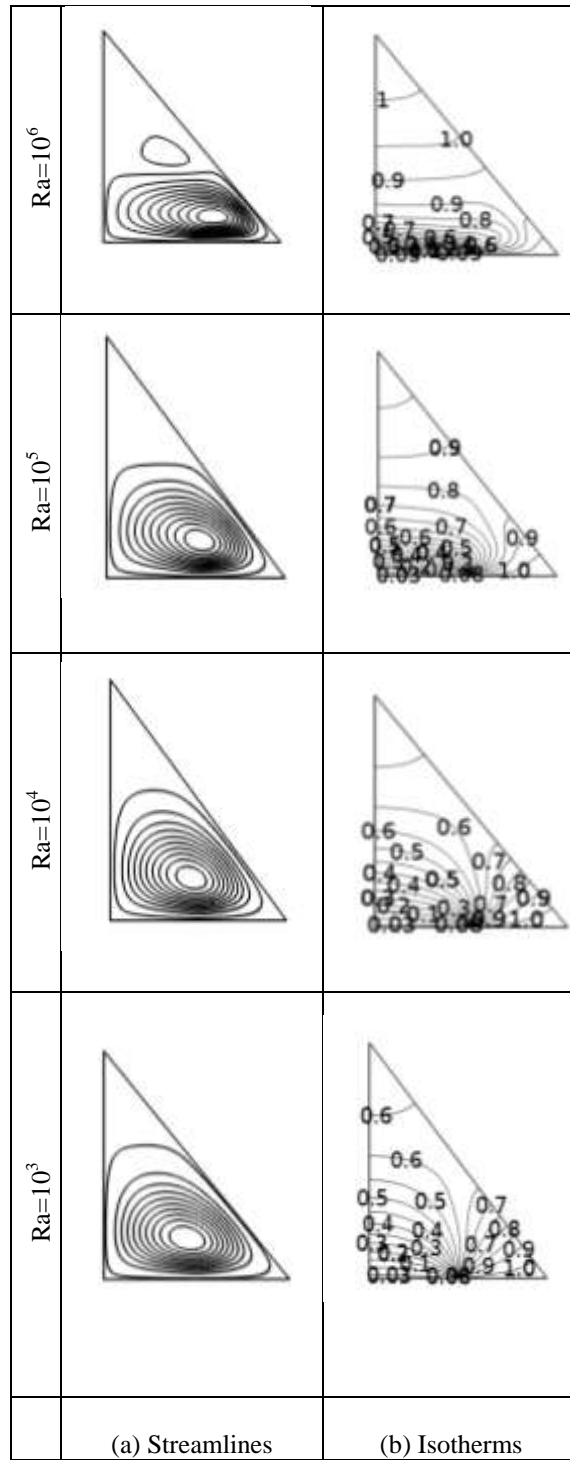


Figure 2: Streamlines and isotherms for different values of Ra when  $\phi = 0.05$ ,  $Q = 1$ , and  $Ha = 25$

Figure 3: Streamlines and isotherms for different values of  $Q$   $\phi = 0.05$ ,  $Ha = 25$ , and  $Ra = 10^6$



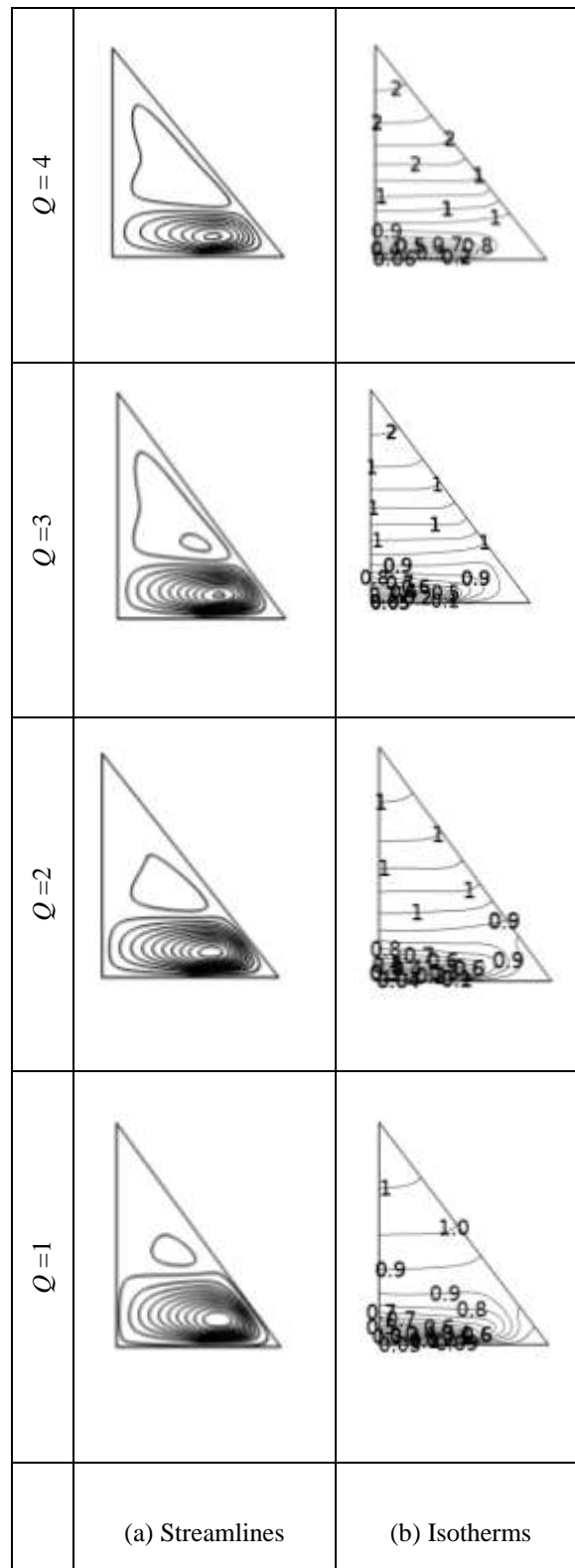


Figure 4: Streamlines and isotherms for different values of Ra when  $\phi = 0.05$ ,  $Q = 1$ , and  $Ha = 25$

Figure 5: Streamlines and isotherms for different values of  $Q$  when  $\phi = 0.05$ ,  $Ha = 25$ , and  $Ra = 10^6$

**Case II: Left cooled (Sink), Right heated (source)**

The influence of Ra and Q are discussed here when the left portion cooled (acting as a sink) and the right portion heated (acting as a source) of the bottom wall of the triangular enclosure. This case is described in Figure 4 and Figure 5.

**Effect of RayleighNumber Ra**

Rayleigh Number (Ra) = 10<sup>3</sup>: At low Rayleigh numbers, the buoyancy forces are relatively weak compared to the viscous forces. As a result, the flow tends to be laminar and steady. The isotherms are relatively smooth, and the streamlines are organized and not significantly affected by convective currents.

Rayleigh Number (Ra) = 10<sup>4</sup>: As the Rayleigh number increases, the buoyancy forces become more dominant compared to viscous forces. The flow may transition from a purely laminar flow to a more complex pattern. The isotherms start to show some irregularities, and convective cells may form, leading to the appearance of more distinct streamlines.

Rayleigh Number (Ra) = 10<sup>5</sup>: At this range of Rayleigh numbers, the buoyancy forces become even stronger, leading to more vigorous fluid motion and the formation of multiple convective cells. The isotherms become more distorted, and the streamlines are no longer smooth lines but rather a complex network of flow patterns.

Rayleigh Number (Ra) = 10<sup>6</sup>: At high Rayleigh numbers, the buoyancy forces dominate the fluid behavior, leading to chaotic and turbulent flow patterns. Convection becomes intense, and the isotherms and streamlines become highly distorted and irregular.

**Effect of Heat Generating Parameter Q**

Heat Generating Parameter (Q) = 1: At Q = 1, the heat generated within the enclosure is relatively low compared to the heat input from the heated side. The main driving force for fluid flow and temperature distribution will be the temperature difference between the heated and cooled sides. The streamlines will exhibit a pattern of convection cells, with fluid rising near the heated side, moving towards the cooled side, and sinking down. The isotherms will show a gradual transition from the heated side to the cooled side, with relatively smooth contours.

Heat Generating Parameter (Q) = 2: As Q increases to 2, the heat generated within the enclosure becomes more significant. It starts to influence the fluid flow and temperature distribution, in addition to the temperature difference between the sides. The streamlines may exhibit more complex patterns with the combined influence of the heat source and the temperature difference. The isotherms will show more variations and steeper temperature gradients within the enclosure.

Heat Generating Parameter (Q) = 3: At Q = 3, the internal heat generation further enhances its impact on the fluid flow and temperature distribution. The streamlines may show turbulent behavior or the formation of multiple convection cells due to the increased heat input. The isotherms will exhibit irregularities and more pronounced temperature gradients, reflecting the stronger influence of the heat source.

Heat Generating Parameter (Q) = 4: At Q = 4, the internal heat generation is even higher. The fluid flow patterns will be significantly influenced by the heat generated within the enclosure. The streamlines may become highly irregular and turbulent, with multiple convection cells dominating the flow. The isotherms will exhibit even more pronounced temperature variations, showing the strong influence of the heat source.

Average Nusselt number for the variation of Ra and Q are tabulated in table 6 and 7 respectively, that shows that heat transfer rate improves for higher values of Ra and Q except for the case of source and Q.

Finally, a comparison in terms of Nu<sub>av</sub> is presented for the location of heat source and sink in table 8 and 9 with varying the magnetic field parameter Ha. One can easily be seen that when Ha increases average Nusselt number decreases except the right sided sink.

**Table no 6:**Average Nusselt number for variation of Ra (L cooled, R heated) while φ = 0.05, Q=1, and Ha= 25

Ra	Nu <sub>c</sub>	Nu <sub>h</sub>
10 <sup>3</sup>	5.3129	4.2787
10 <sup>4</sup>	5.3794	4.3389
10 <sup>5</sup>	6.2168	5.1408
10 <sup>6</sup>	8.4042	7.2586

**Table no 7:**Average Nusselt number for variation of Q (L cooled, R heated) while φ = 0.05, Ha= 25, and Ra = 10<sup>6</sup>

Q	Nu <sub>c</sub>	Nu <sub>h</sub>
1	8.4042	7.2586
2	8.8807	6.7045
3	9.3716	6.1744
4	9.8836	5.7031

**Table no 8:** Comparison of location of source while  $\phi = 0.05$ ,  $Q=1$ ,  $Ha= 25$  and  $Ra = 10^6$  (left and right source)

Ha	$(Nu_h)_L$	$(Nu_h)_R$
0	1.0246	7.3838
25	1.0245	7.2586
50	1.0241	6.9620
100	1.0228	6.2027

**Table no 9:** Comparison of location of sink while  $\phi = 0.05$ ,  $Q=1$ ,  $Ha= 25$  and  $Ra = 10^6$  (left and right sink)

Ha	$(Nu_c)_L$	$(Nu_c)_R$
0	8.5306	0.3208
25	8.4042	0.3284
50	8.1054	0.3457
100	7.3381	0.3828

### V. Conclusions

A two-dimensional study is carried out herein to expose the flow patterns and heat transfer manner of anelectrically conducting fluid subjected to externally imposed magnetic field along with heat source and sink at bottom wall of a triangle shaped cavity. In view of the obtained results, the following conclusions may be summarized.

- It was found that the Rayleigh number plays a vital role on both streamlines and isotherms with the increasing value of Rayleigh number, enhance the average Nusselt number.
- For the higher values of heat generation parameter, average Nusselt number increases for sink and reduces for source.
- It was also observed that the magnetic field has a significant impact on the fluid flow and temperature distribution following the reverse effect.

### References

- [1]. Rashad AM, Chamkha AJ, Ismael MA, Salah Taha. MHD natural convection in a triangular cavity filled with a Cu-Al<sub>2</sub>O<sub>3</sub>/water hybrid nanofluid with localized heating from below and internal heat generation. J. of Heat Transfer. 2018, pp. 1-23 (doi:10.1115/1.4039213).
- [2]. Dogonchi AS , Ismael MA and Chamkha AJ. Numerical analysis of natural convection of Cu- water nanofluid filling triangular cavity with semicircular bottom wall. J Therm Anal calorim . 2019; 135, 3485-3497.
- [3]. Mahmoudi A, Pop I and Shahi M . Effect of magnetic field on natural convection in a triangular enclosure filled with nanofluid. *Int. J. Therm. Sci.* **2012**, 59, 126–140.
- [4]. Chamkha and Ismael . Magnetic field effect on mixed convection in LID-driven trapezoidal cavities filled with a Copper–Water nanofluid with an aiding or opposing side wall. J Thermal Sci .Engg. App. 2016, 8, pp-031009 - 1 .
- [5]. Angirasa D. Analysis of hybrid nanofluid behavior in a triangular cavity along with heat source considering the effect of Magnetic force. Fluid Dynamics Research . 2000, vol.26. pp.219-233.
- [6]. Kadhim HT, Jabbar FA and Rona A . Cu-Al<sub>2</sub>O<sub>3</sub> hybrid nanofluid natural convection in an inclined enclosure with wavy walls partially layered by porous medium . *Int. J. Mech. Sci.* **2020**, 186, 105889.
- [7]. Khanafer Vafai K and Lightstone M. Buoyancy driven heat transfer enhancement in a two-dimensional enclosure utilizing nanofluids. Int. J Heat Mass Transfer. 2003, 446, pp.3639-3653.
- [8]. Garud KS and Lee MY. Numerical investigations on heat transfer characteristics of single particle and hybrid nanofluids in uniformly heated tube. *Symmetry*. **2021**, 13, 876.
- [9]. Tawfik MM .Experimental studies of nanofluid thermal conductivity enhancement and applications :A review. Renew sust. Energ. 2017; 75: 1239-1253.
- [10]. Muhammad MJ , Mahammad IA , Sidik NAC, Yazid MNAW ,Mamat R and NajaFi G .The use of nanofluids for enhancing the thermal performance of stationary solar collectors: A review. Renew Sust. Energ. 2016; 63, 226-236.
- [11]. Raja RB, Vijayan R ,Dinesh KP and Venkatesan M . Review on nanofluids characteristics, heat transfer characterization and applications. Renew sust. Energ. 2016; 64, 163-173.
- [12]. Botha SS , dungu PN and Bladergroen BJ. physicochemical properties of oil based nanofluids containing hybrid structures of silver nanoparticle supported on silica. Ind.Eng.chem,Res .2011, 50, pp.3071-3077.
- [13]. You SM, Kim JH and Kim KH. Effect of nanoparticles on critical heat flux of water in pool boiling heat transfer. Applied physics letters, 2003, vol.83, no.16, pp.3374-3376.
- [14]. Tayebi T, Oztop HF and Chamkha AJ. Natural convection and entropy production in hybrid nanofluid filled-annular elliptical cavity with internal heat generation or absorption. Therm. Sci. Eng. Prog. 2020, vol. 19, pp. 100605.
- [15]. Azmi WH, Sharma KV, Mamat R, Najafi G and Mohamad MS. The enhancement of effective thermal conductivity and effective dynamic viscosity of nanofluids: A review. Renew.sust. Energ. 2016; 53, 1046-1058.
- [16]. H.C. Brinkman. The viscosity of concentrated suspensions and solution. J. Chem 20. 1952, pp 571-581.
- [17]. J.C. Maxwell. A treatise on electricity and magnetism. Oxford, UK: Clarendon Press. 1873.